

Frequency response in surface-potential driven electro-hydrodynamics

L. E. Jørgensen, K. Smistrup, C. M. Pedersen, N. A. Mortensen, and H. Bruus

MICRO Department of Micro and Nanotechnology,

Technical University of Denmark, NanoDTU Bldg. 345 east, DK-2800 Kongens Lyngby, Denmark

(dated: February 9, 2006)

Using a Fourier approach we offer a general solution to calculations of slip velocity within the circuit description of the electro-hydrodynamics in a binary electrolyte confined by a plane surface with a modulated surface potential. We consider the case with a spatially constant intrinsic surface capacitance where the net flow rate is in general zero while harmonic rolls as well as time-averaged vortex-like components may exist depending on the spatial symmetry and extension of the surface potential. In general the system displays a resonance behavior at a frequency corresponding to the inverse RC time of the system. Different surface potentials share the common feature that the resonance frequency is inversely proportional to the characteristic length scale of the surface potential. For the asymptotic frequency dependence above resonance we find a ω^{-2} power law for surface potentials with either an even or an odd symmetry. Below resonance we also find a power law ω^{-1} with ω being positive and dependent of the properties of the surface potential. Comparing a tanh potential and a sech potential we qualitatively find the same slip velocity, but for the below-resonance frequency response the two potentials display different power law asymptotics with ω^{-1} and ω^{-2} , respectively.

PACS numbers: 47.65.+a, 47.32.-y, 47.70.-n, 85.90.+h

I. INTRODUCTION

The ability to manipulate liquids on microfluidic chips is essential to the functionality of micrototal analysis systems [1] and recently there has been quite some interest in utilizing AC electrical surface potentials for pumping, manipulating, and mixing electrolytes. For an overview of electro-hydrodynamics and AC electro-osmosis we refer to Refs. 2, 3, 4, 5, 6, 7, 8, 9 and references therein.

In this paper we consider the RC model in Ref. 3 of an electrolyte confined by an insulating surface with an applied external potential of the general form

$$V_{\text{ext}}(y;t) = V_0 f(y) \exp(i\omega t) \quad (1)$$

Here, ω is the driving frequency and $f(y)$ is a dimensionless function representing the amplitude variations along the surface. For simplicity we consider a binary electrolyte with permittivity ϵ , viscosity η , and conductivity σ . Assuming a low Peclet number we may neglect convection so that the electrohydrodynamics can formally be solved independently of the hydrodynamics. On the other hand the hydrodynamics of course still depends on the electrohydrodynamics through the body force which effectively may be taken into account through a finite slip velocity, see e.g. Refs. 3, 7, 10, 11, 12 and references therein.

II. ELECTRODYNAMICS

For the electrohydrodynamics we follow Ajdari [3] with the surface and the Debye layer each represented by a capacitive element while the bulk-liquid is represented by an ohmic element. The model applies to the situation where spatial variations along the surface are slow on the

length scale of the Debye screening length λ_D , the driving frequency is small compared to the Debye frequency ω_D , and the electrostatic energy is small compared to the thermal energy $k_B T$, i.e. the Debye-Hückel approximation is valid. As shown by many, the model may be justified in detail starting from a non-equilibrium electrohydrodynamic continuum description. For more details we refer to Refs. 10, 11 as well as 8, 9 and references therein.

In the bulk of the liquid there is charge neutrality and the electrical potential thus fulfills the Laplace equation $\nabla^2 \phi = 0$ subject to the relation between surface charge ρ_D and the potential drop across the capacitive element $\phi(0;y;t) - V_{\text{ext}}(y;t) = \lambda_D \rho_D$ as well as a continuity equation $\partial_t \rho_D(y;t) = -\nabla_x J_x(0;y;t) = -\partial_x \phi(x=0;y;t)$ relating the change in surface charge to the electrical Ohmic current J . Above, $C_0 = C_s^{-1} + C_D^{-1}$ is a series capacitance with C_s being the intrinsic surface capacitance and $C_D = \epsilon/\lambda_D$ being the Debye layer capacitance.

We formally solve this problem by introducing the inverse Fourier transform $F(Q)$ of $f(y)$, see Eq. (1),

$$F(Q) = \int_{-\infty}^{\infty} \frac{dy}{2\pi} f(y) e^{iQy} \quad (2)$$

From the solution of the spatially harmonic problem [3] we may write the general solutions for the potential and the surface charge as

$$\phi(x;y;t) = V_0 \exp(i\omega t) \int_{-\infty}^{\infty} \frac{dQ}{2\pi} \frac{F(Q) \exp(iQy) \exp(-Qx/\lambda_D)}{1 - i\omega/\omega_D} \quad (3)$$

and

$$D(\mathbf{y};t) = i \frac{V_0}{\omega} \exp(i\omega t) \int_0^{\omega} \frac{dQ}{2} \frac{F(Q) \mathcal{D} \exp(iQy)}{1 + iQj_D} : \quad (4)$$

Above, we have introduced the frequency dependent effective length scale D given by

$$D = (1 + \frac{1}{\omega} \frac{C_D}{C_S})^{-1} D_0 ; \quad (5)$$

where $\frac{C_D}{C_S}$ is the capacitance ratio and $\omega_D = \frac{D_0}{b}$ is the Debye frequency.

III. THE SLIP VELOCITY

The slip velocity is given by [3]

$$v_{\text{slip}}(\mathbf{y}) = \frac{D}{\omega} \frac{h}{\omega} \frac{i}{\omega} \mathcal{G}_y(\mathbf{x};\mathbf{y})_{x=0} ; \quad (6)$$

where it is implicit that real values of D and ω must be taken. From Eqs. (3) and (4) we now formally get

$$v_{\text{slip}}(\mathbf{y};t) = \frac{D}{\omega} \frac{V_0^2}{\omega} \frac{1}{\omega} \int_0^{\omega} \frac{dQ}{2} \frac{F(Q) \mathcal{D} \exp(iQy)}{1 + iQj_D} \text{Re} \{ e^{i\omega t} \} \\ + \frac{D}{\omega} \frac{V_0^2}{\omega} \frac{1}{\omega} \int_0^{\omega} \frac{dQ^0}{2} \frac{F(Q^0) Q^0 \exp(iQ^0 y)}{1 + iQ^0 j_D} \text{Re} \{ e^{i\omega t} \} ; \quad (7)$$

and for the time-averaged slip-velocity v_{slip_t} we use that $\text{Re} \{ e^{i\omega t} \} \text{Re} \{ e^{i\omega t} \} = \frac{1}{2} \text{Re} \{ e^{i\omega t} e^{-i\omega t} \}$ as well as $F(Q) = F(Q^0)$ so that

$$v_{\text{slip}}(\mathbf{y};t)_t = \frac{D}{\omega} \frac{V_0^2}{\omega} \frac{1}{\omega} \text{Re} \left\{ \int_0^{\omega} \frac{dQ}{2} \frac{F(Q) \mathcal{D} \exp(iQy)}{1 + iQj_D} \int_0^{\omega} \frac{dQ^0}{2} \frac{F(Q^0) Q^0 \exp(iQ^0 y)}{1 + iQ^0 j_D} \right\} : \quad (8)$$

Eqs. (7) and (8) are our general results for the surface-potential induced hydrodynamics. Velocity and pressure fields may be obtained by solving the Navier-Stokes equation without body-forces subject to a slip-velocity condition.

Before turning our attention to specific potentials we may already extract some general properties of the model. From Eq. (8) it is clear that $v_{\text{slip}}(\mathbf{y};t)_t$ is a spatially dependent function of finite magnitude. This in turn also means that the external potential can induce a finite time-averaged velocity field in the fluid. However, it is also clear that the induced net flow rate will be zero since $v_{\text{slip}}(\mathbf{y};t)_t$ has no spatial dc-component, as may

be seen by substituting the general expression for $F(Q)$. Spatial asymmetry in the applied potential is thus not a sufficient condition to achieve pumping and as also indicated in Ref. 3, asymmetry in the surface capacitance is required. Formal studies of the model for $\epsilon_y C_S \neq 0$ will be an interesting subject for future studies, but here we will follow the lines where C_S is constant along the surface. The case of $f(y) = \cos(qy)$ was first studied in Ref. 3. The Fourier transform is then a simple sum of two Dirac delta functions, $F(Q) = \delta(Q - q) + \delta(Q + q)$, and substituting into Eqs. (7) or (8) we easily arrive at results fully consistent with those reported previously.

IV. FREQUENCY DYNAMICS

In order to draw some general conclusions about the frequency dynamics of the hydrodynamics, apart from the frequency doubling [3], we imagine that the surface potential has a characteristic length scale $l = q$. Since we have made an RC description of the electrohydrodynamics it follows quite naturally that the system will have a resonance behavior at a frequency comparable to the inverse RC time of the system. Above resonance the system has an asymptotic power-law frequency response as we will illustrate below for a surface potential of even symmetry. In that case $F(Q)$ is a real and even function of Q , so that Eq. (8) with $Q = sq$ becomes

$$v_{\text{slip}}(\mathbf{y};t)_t = 2v_q^2 \text{Re} \left\{ \int_0^{\omega} \frac{ds}{2} \frac{F(sq) s \cos(sqy)}{\frac{1}{\omega} + is} \right\} \\ + \int_0^{\omega} \frac{ds^0}{2} \frac{i \frac{1}{\omega} F(s^0 q) s^0 \sin(s^0 qy)}{\frac{1}{\omega} + is^0} ; \quad (9)$$

where we have introduced a characteristic resonance frequency ω as well as a characteristic flow velocity v_q ,

$$\omega = q D (1 + \frac{1}{\omega} \frac{C_D}{C_S})^{-1} D_0 = q D_0 ; \quad v_q = \frac{q V_0^2}{(1 + \frac{1}{\omega} \frac{C_D}{C_S})} ; \quad (10)$$

Since

$$\text{Re} \left\{ \frac{1}{is + \frac{1}{\omega}} \right\} = \frac{(s^0 - s)^2}{[\omega^2 + s^2][\omega^2 + (s^0)^2]} \\ = (s - s^0)^2 + O(\omega^{-4}) \quad (11)$$

we expect with $\omega = \omega$ that

$$v_{\text{slip}_t} / \omega^2 ; \quad \omega \rightarrow \omega : \quad (12)$$

Likewise, for surface potentials of odd symmetry we arrive at the same conclusion. Making a similar expansion for the below-resonance asymptote one might speculate that $v_{\text{slip}_t} / \omega$ with a power $\alpha = 2$. However, with such an expansion the integrals are in general no longer convergent which in turn indicates that the power α is below 2 depending on the actual surface potential under consideration. In the following we will illustrate this by the aid of two explicit examples.

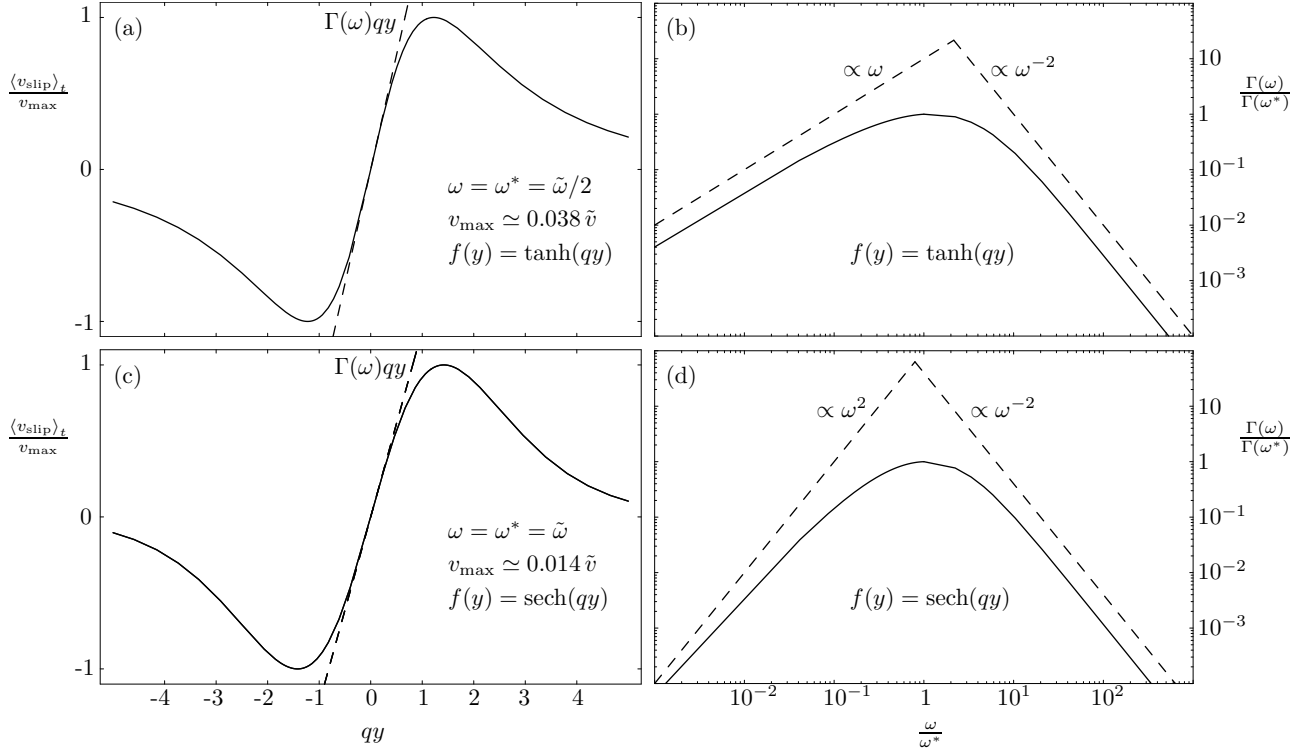


FIG. 1: Dynamics for $\tanh(qy)$ and $\text{sech}(qy)$ surface potentials, panels (a)–(b) and (c)–(d), respectively. Panels (a) and (c) show the time-averaged slip velocities at resonance while panels (b) and (d) show the corresponding frequency response. In (a) and (c) the solid lines show numerical evaluations of Eqs. (13) and (15), respectively, while dashed lines show the slope $\partial_y v_{\text{slip}}|_{t=y=0}$ at $y = 0$ calculated from Eqs. (14) and (16), respectively. In (b) and (d) the solid lines show numerical evaluations of Eqs. (14) and (16), respectively, while dashed lines are included to indicate asymptotics.

A. Two-electrode configuration

Recently, a circulating flow was observed experimentally using two adjacent electrodes and an AC field [12] and in Ref. [13] the problem was studied theoretically by assuming that the two electrodes are infinitely close corresponding to a step-like model potential. However, such a potential is somewhat unphysical since the electric field diverges and instead one should take the electrode gap into account [14]. In the following we model such an electrode configuration with a smooth external potential of the form $f(y) = \tanh(qy)$ which incorporates the built-in electrode gap in terms of the length scale $l=q$. Fourier transforming and substituting into Eq. (8) we get

$$v_{\text{slip}}(y;t)_t = v \text{Re} \left(\int_0^Z ds \frac{\text{csch}(\frac{1}{2}s) s \sin(sqy)}{i_1^{-1} + 2s} \right) \int_0^Z ds^0 \frac{i_1^{-1} \text{csch}(\frac{1}{2}s^0) s^0 \cos(s^0 qy)}{i_1^{-1} - 2s^0}; \quad (13)$$

where the resonance frequency is given by $\omega = \omega^* = 2$. In order to study the maximal value of $v_{\text{slip}}(y;t)_t$ as a function of frequency we note that when $v_{\text{slip}}(y;t)_t$ is maximal so is its slope at $y = 0$. If we define $\Gamma(\omega) =$

$(qv)^{-1} \partial_y v_{\text{slip}}(y;t)|_{t=y=0}$ we get

$$= 2^{-2} (J_2^2 - J_1 J_3); \quad J_n = \int_0^Z ds \frac{\text{csch}(\frac{1}{2}s) s^n}{2 + 4s^2} \quad (14)$$

where we have introduced $\omega = \omega^* = 2$. Panel (a) of Fig. 1 shows the time-averaged slip velocity at resonance evaluated numerically from Eq. (13) and its slope at $y = 0$, based on a numerical evaluation of Eq. (14), is also included. Panel (b) shows $\Gamma(\omega)$ as a function of frequency. The plot confirms Eq. (12) and suggests a linear dependence $v_{\text{slip}}|_{t=y=0} / \omega$ for the below-resonance frequency response. This may also be confirmed by an asymptotic analysis by first noting that $J_1 \approx 1 - \frac{1}{2} \ln(2) + O(\omega^{-2})$. For J_2 we note that $\partial J_2 = \partial \int_0^Z ds \text{csch}(\frac{1}{2}s) s^2 = \int_0^Z ds s^2 [2 + 4s^2]^{-2}$, $\partial J_2 = \frac{1}{4} \int_0^Z ds s^2 [2 + 4s^2]^{-2} = \frac{1}{8} \int_0^Z ds s^2 [2 + 4s^2]^{-2}$ so that $\partial J_2 = \text{const}$: $\ln(2) = 2$. For J_3 we similarly note that $\partial J_3 = \partial \int_0^Z ds s^3 \text{csch}(\frac{1}{2}s) = \text{const}$: $\ln(2) = 8$. When collecting terms we thus get a ω^{-2} dependence to lowest order.

B. Single-electrode configuration

As a second example we consider single-electrode driven electrohydrodynamics and as a model potential

we use $f(y) = \text{sech}(qy)$ to mimic the potential of a single electrode with a characteristic width $l=q$. Fourier transforming and substituting into Eq. (8) we get

$$v_{\text{slip}}(y;t) = \frac{1}{2} \text{Re} \int_0^{Z_1} ds \frac{i_1^{-1} \text{sech}(\frac{1}{2}s) \cos(s^0 qy)}{i_1^{-1} + s} \int_0^{Z_1} ds^0 \frac{\text{sech}(\frac{1}{2}s^0) s^0 \sin(s^0 qy)}{i_1^{-1} - s^0}; \quad (15)$$

where in this case $\omega = \omega$ is the resonance frequency. In analogy with the previous example we get

$$= \frac{1}{2} \omega^2 (I_2^2 - I_1 I_3); \quad I_n = \int_0^{Z_1} ds \frac{\text{sech}(\frac{1}{2}s) s^n}{2 + s^2} \quad (16)$$

Panel (c) in Fig. 1 shows the time-averaged slip velocity at resonance evaluated numerically from Eq. (15) and the slope at $y = 0$ based on a numerical evaluation of Eq. (16) is also included. Panel (d) shows the frequency response comparing Eq. (12) for the above-resonance response while for the below-resonance response $v_{\text{slip}}(y;t) / \omega$ with a power ω^{-2} . For the asymptotic analysis we note that $I_2 = 1 + O(\omega^{-2})$ and $I_3 = 8C = \omega^{-2} + O(\omega^{-4})$ where $C = 0.915966$ is Catalan's constant. For I_1 it follows that $\int_0^{Z_1} ds \text{sech}(\frac{1}{2}s) s = \int_0^{Z_1} ds \frac{1}{2 + s^2} = \frac{1}{2} \ln(2 + Z_1^2) + O(\omega^{-2})$. There will thus be a logarithmic correction $\omega^{-2} \ln(\omega)$ to the ω^{-2} dependence.

V. DISCUSSION AND CONCLUSION

In this work we have used a Fourier transform approach to make a general analysis of the frequency dynamics of AC-induced electrohydrodynamics within the RC model

of Ref. 3. In the case with a spatially constant intrinsic surface capacitance we generally prove that the net flow rate is zero. A finite net flow rate will require a spatially inhomogeneous capacitance so that the charge and electrical field dynamics are mutually out of phase.

For the frequency dynamics we observe a resonance behavior at a frequency corresponding to the inverse RC time of the system and different surface potentials share the common feature that the resonance frequency is inversely proportional to the characteristic length scale of the surface potential. Above resonance we in general find a ω^{-2} power law for surface potentials with either even or odd symmetry. Below resonance we likewise find a power-law dependence ω with ω being positive and dependent of the properties of the surface potential. As two examples we have compared \tanh (odd symmetry) and sech (even symmetry) surface potential. Unexpectedly, we qualitatively find the same slip velocity, while the frequency dynamics is very different for the below-resonance frequency response where power law asymptotics with $\omega = 1$ and ω^{-2} , respectively, are found.

Our study illustrates how the frequency dynamics carries strong fingerprints of the driving surface potential and we believe that detailed analysis of the frequency dynamics would be a way to extract more information from experimental data. Recent related work [15] also suggests the possibility for a strong frequency dependence in ac electroosmosis also in the flow topology.

Acknowledgement

We thank L. H. Olesen for stimulating discussions. K.S. is supported by CONIT and Teknologisk Institut. N.A.M. is supported by The Danish Technical Research Council (Grant No. 26-03-0073).

-
- [1] O. G. Eschke, H. K. Lank, and P. Telieps, eds., *Microsystem Engineering of Lab-on-a-Chip Devices* (Wiley-VCH Verlag, Weinheim, 2004).
- [2] A. Ramos, H. M. Organ, N. G. Green, and A. Castellanos, *J. Phys. D Appl. Phys.* 31, 2338 (1998).
- [3] A. Ajdari, *Phys. Rev. E* 61, R45 (2000).
- [4] H. M. Organ and N. G. Green, *AC Electrokinetics: colloids and nanoparticles, Microtechnologies and Microsystem series* (Institute of Physics Publishing, Bristol, 2003).
- [5] H. A. Stone, A. D. Stroock, and A. Ajdari, *Annu. Rev. Fluid Mech.* 36, 381 (2004).
- [6] M. Z. Bazant and T. M. Squires, *Phys. Rev. Lett.* 92, 066101 (2004).
- [7] T. M. Squires and M. Z. Bazant, *J. Fluid Mech.* 509, 217 (2004).
- [8] M. Z. Bazant, K. Thornton, and A. Ajdari, *Phys. Rev. E* 70, 021506 (2004).
- [9] N. A. Mortensen, L. H. Olesen, L. Behnke, and H. Bruus, *Phys. Rev. E* 71, 056306 (2005).
- [10] N. I. Gamayunov, V. A. Murtsovkin, and A. S. Dukhin, *Kolloidn. Zh.* 48, 233 (1986).
- [11] V. A. Murtsovkin, *Kolloidn. Zh.* 58, 358 (1996).
- [12] N. G. Green, A. Ramos, A. Gonzalez, H. M. Organ, and A. Castellanos, *Phys. Rev. E* 61, 4011 (2000).
- [13] A. Gonzalez, A. Ramos, N. G. Green, A. Castellanos, and H. M. Organ, *Phys. Rev. E* 61, 4019 (2000).
- [14] A. Ramos, A. Gonzalez, A. Castellanos, N. G. Green, and H. M. Organ, *Phys. Rev. E* 67, 056302 (2003).
- [15] J. A. Levitan, S. D. Evasenathipathy, V. Studer, Y. X. Ben, T. Thorsen, T. M. Squires, and M. Z. Bazant, *Colloid Surf. A Physicochem. Eng. Asp.* 267, 122 (2005).